Vortex/Separated Boundary-Layer Interactions at Transonic Mach Numbers

Rabindra D. Mehta*
Stanford University, Stanford, California

An experimental study has been completed on the effect of a single longitudinal vortex on a separated, transonic, turbulent boundary layer. The vortex was generated by a half-delta wing mounted at the upstream end of an axisymmetric "bump" model. A flow visualization study was conducted using vapor screen and surface oilflow techniques. In addition surface pressures were measured and mean flow and turbulence data obtained using a two-component laser velocimeter. At precritical Mach numbers, the vortex delayed or eliminated boundary-layer separation on the downwash side and enhanced it on the upwash side, thus converting a nominally two-dimensional separation into a three-dimensional one. At the postcritical Mach number, the effect of the vortex was to reduce the size and extent of the shock-induced boundary-layer separation throughout the region of interaction. The boundary-layer turbulence in both cases was found to reorganize accordingly, although in a rather complex manner. The onset of three-dimensionality in the separation line produced by the vortex resulted in secondary vortices (foci), the sign and number being strongly dependent on the freestream Mach number.

Nomenclature

c	= bump chord
C_p	= pressure coefficient, $(p-p_\infty)/\frac{1}{2}\rho U_\infty^2$
F,N,S	= critical points; focus, node, and saddle, respectively
h	= semispan (height) of vortex generator
l	= root chord (length) of vortex generator
M	= freestream Mach number
p	= static pressure
p_∞	= reference static pressure in the test section
Re	= Reynolds number
R_{uv}	= shear correlation coefficient, $-\overline{u'v'}/\sqrt{\overline{u'^2}}\sqrt{\overline{v'^2}}$
R_Γ	= vortex circulation Reynolds number, Γ/ν
U,V,W	= mean velocity in the X,Y,Z directions, respectively
U_∞	= reference freestream velocity in the test section
u',v',w'	= fluctuating velocity components in the X,Y,Z directions, respectively
u,v,w	= instantaneous velocity in the X,Y,Z directions, respectively, e.g., $u=U+u'$
X,Y,Z	= Cartesian coordinates for streamwise, normal, and spanwise directions, respectively
α	= vortex generator angle of attack
δ_{995}	= boundary-layer thickness
Γ	= overall vortex circulation
ν	= kinematic viscosity
ρ	= density
$\bar{(\ )}$	= time-averaged quantity

Introduction

THE principle of boundary-layer separation control by vortex generators has been known and used on aircraft wings since the 1940's. It involves the generation of discrete longitudinal vortices near the surface so that mixing between the higher momentum external stream and the boundary layer is increased. However, with higher demands on aircraft performance in recent years, attention has also been focused on the interaction between a single, relatively strong vortex and the wing boundary layer and wake. One situation of particular interest is when the longitudinal vortex interacts with a separated boundary layer. Such interactions are becoming increasingly important in advanced aircraft technology: highly maneuverable fighter aircraft utilize the vortex from a canard or strake to suppress or control boundary-layer separation on the wing so that the necessary stability is sustained. Another example is in rotorcraft, where the blade goes through phases when the boundary layer is separated, and this is then acted upon by the tip vortex shed from the blade ahead. In both cases, transonic speeds are often achieved where the separation is induced by the presence of a shock wave. It is essential to obtain detailed and accurate measurements in such complex interactions if our basic understanding is to be improved so that new turbulence models and hence calculation methods may be developed. At present, our understanding and predictive capability for such complex flows, where the turbulence is no longer in equilibrium, is very limited, as evidenced at the recent Stanford Conference on Complex Turbulent Flows.[1]

Some recent results from experimental investigations have indicated the level of complexity encountered in such interactions. In a detailed study of a longitudinal vortex imbedded in a two-dimensional turbulent boundary layer,[2] it was found that the turbulence structure was altered drastically. The eddy viscosities defined for the different shear-stress components behaved in different, and complicated, ways. Terms in the Reynolds-stress transport equations, notably the triple products that affect turbulent diffusion of Reynolds stress, also failed to obey simple rules. The results suggested that simple empirical turbulence models for these quantities may not yield predictions accurate in detail. This reservation gained some support from the recent computational attempts of Liandrat et al.,[3] who found that while the overall mean flow properties were adequately predicted using a mixing-length model, the Reynolds shear stresses, for example, were predicted very poorly. In another experimental vortex/boundary-layer study,[4] the effects of an adverse pressure gradient on the vortex and the interaction were investigated. It was found that the primary effect of the adverse pressure gradient was to accelerate the growth of the vortex core which caused the vortex shape to become more

Received Nov. 19, 1986; revision received April 13, 1987.

*Research Associate, Department of Aeronautics and Astronautics, Joint Institute for Aeronautics and Astronautics.

elliptic. The possibility of vortex "meander" causing this ellipticity has also been investigated.[5] An additional effect of the pressure gradient was to induce stronger distortions in the Reynolds-stress distributions. In the extreme case, a sufficiently strong adverse pressure gradient can lead to vortex breakdown. On a delta wing, for example, the pressure gradient decelerates the flow along the vortex centerline until a stagnation point appears, followed by a limited region of reversed axial flow.[6] This leads to either a "bubble-type" or "spiral-type" breakdown of the vortex. In passage through a shock wave, a similar effect is produced, although vortex breakdown only occurs for critical values of vortex and shock strength.[7] A weaker shock increases the rate of swirl and decelerates the core flow, thus making the vortex more vulnerable to breakdown.

The present investigation is one of a series primarily designed to improve our understanding of vortex/shear flow interactions.[8] Flows of practical interest are investigated in simplified and controlled situations so that individual effects can be identified and studied. The main objective of the present investigation was to study the effect of a single longitudinal vortex on a nominally two-dimensional separated turbulent boundary layer, with emphasis on departure from accepted two-dimensional behavior. In particular, details of the changes in boundary-layer turbulence induced by the vortex were to be established. The undisturbed (without the vortex) shock-induced separation on this model was previously investigated by Bachalo and Johnson.[9] For the present study, a vortex generator was mounted at the model leading edge. Some selected results from the investigation are presented in this paper. Additional data at other streamwise locations, including some in the reattached region, are given in Ref. 10 for the precritical case and in Ref. 11 for the postcritical case; a complete set of tabulated data is also available from the author.

Experimental Apparatus and Techniques

The experiments were conducted in the NASA Ames 2×2 ft (61×61-cm) transonic wind tunnel. The facility is a closed-return, variable-density, continuously operating tunnel with 21% open porous-slotted upper and lower walls. The axisymmetric flow model consisted of an annular circular arc bump affixed to a hollow circular cylinder (Fig. 1). The cylinder had a 15.2-cm o.d. with 0.64-cm-thick walls and extended 61 cm upstream of the bump leading edge; the maximum model diameter at the bump apex was 18.9 cm.

The axisymmetric configuration offered several advantages. With the curved surfaces, diffuse reflections of the laser beams from the model surface were reduced, thus allowing measurements to be made to within 0.02 cm of the surface. Sidewall interference problems were also minimized by using an axisymmetric model. Although this does not include blockage effects, for the present model the area blockage was only about 3.5%. Furthermore, previous pressure measurements obtained in the 2×2-ft tunnel were found to agree extremely well with those obtained in the much larger 6×6-ft tunnel.[12] As an additional advantage, the shock wave on the present model terminated before reaching the tunnel walls, thus reducing shock oscillation problems due to interference with the wall boundary layers. Since the ratio of undisturbed boundary-layer thickness to cylinder radius of curvature was ~1:5, the effects due to lateral curvature were not expected to be very large and were therefore neglected in the present analysis.

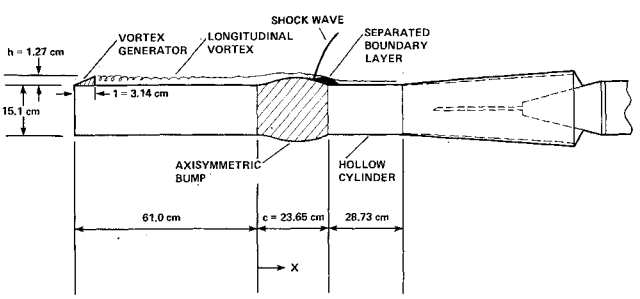

Fig. 1 Schematic of experimental model.

The vortex was generated by a half-delta wing, 1.27-cm semispan and 3.14-cm base-chord, placed at a fixed angle of attack of 15 deg on a 7.62-cm-wide and 0.12-cm-thick band which was mounted at the upstream end of the cylinder model. The leading and trailing edges of the band were tapered in order to minimize boundary-layer disturbance. The band was held by a clamping device which allowed the position of the vortex to be rotated. The semispan of the delta wing was chosen to approximately equal the boundary-layer thickness at the bump leading edge so that the vortex would become imbedded in the boundary layer.

Although the vortex strength could not be determined directly from the present two-dimensional measurements, the V data and observations from previous experiments[2,4] indicated that the maximum crossflow velocities were equivalent to less than 15% of the freestream velocity. The estimated vortex circulation ($\Gamma/U_\infty c$) was about 0.025, giving a vortex Reynolds number (R_Γ) of about 62,500. The generated vortex may therefore be considered to be relatively small and weak compared to typical vortices encountered in practical aerodynamics, such as the strake vortex on a fighter aircraft, which has an R_Γ that is larger by at least an order of magnitude.

A two-component laser velocimeter system was used for the velocity measurements. The system utilized two wavelengths (0.488 and 0.5145 μm) from an argon-ion laser. Bragg cell frequency shifting (40 MHz) was introduced in both lines to reduce the relative frequency bandwidth requirements on the processor when measuring in regions of high turbulence intensity. Frequency shifting also enabled directional discrimination so that reversed-flow regions could be investigated. The optical components used to produce the orthogonal pairs of beams and the Bragg cells were mounted on an optics table located outside the wind tunnel pressure chamber. Mirrors were used to direct the four-beam matrix into the pressure chamber where the transmitting and collecting optics were located. Scattered light was collected in the off-axis forward scatter mode and signal processing was accomplished with single-particle burst counters. Individual realizations from the two channels were multiplexed simultaneously to an HP9845 computer via a NASA-built LDV interface. Two synchronously operated traversing systems with stepping motors were used to position the transmitting and receiving optics. An effective sensing volume was formed by the focused laser beams and the off-axis collection optics that was approximately 200 μm in diameter and 2 mm long, with its major axis normal to the flow direction. The flow was seeded by mounting an ultrasonic spray nozzle, which generated mineral oil droplets with a mean diameter of 0.7 μm, in the settling chamber.

The data presented in this paper were not weighted for velocity biasing. Johnson et al.[13] showed that for the results obtained on this model by Bachalo and Johnson,[9] correcting for velocity bias by weighting each sample inversely to the magnitude of the instantaneous velocity resulted in small changes in the actual measured values, but not enough to affect the overall conclusions. Since in the present investigation the main objective was to study the effect of the vortex, the bias corrections were not implemented.

The model was equipped with a row of pressure taps (a total of 35) along a single streamwise plane which was aligned so that the taps faced the wind tunnel ceiling. Streamwise pressure and velocity profiles at various circumferential positions in the interaction were obtained by rotating the vortex generator position around the model. All the individual velocity profiles were therefore measured in a plane perpendicular to the model surface.

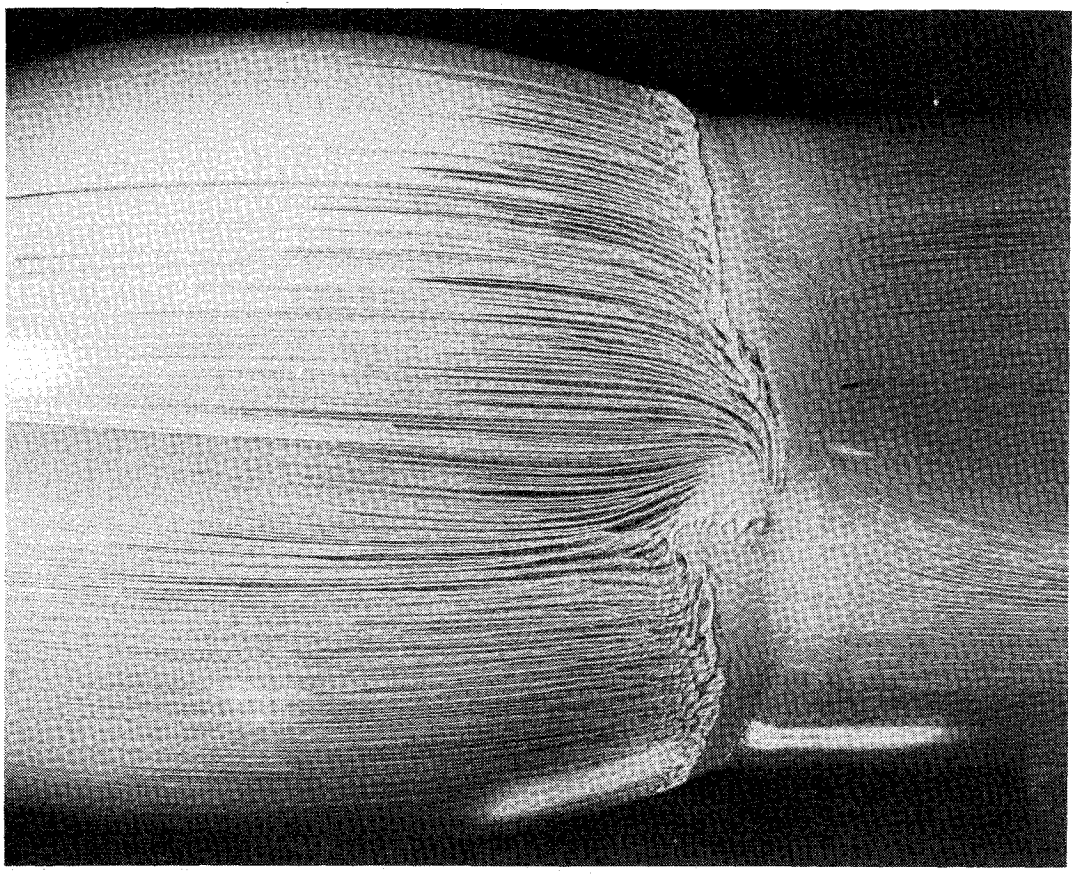

Fig. 2a Oil-flow visualization, $M = 0.7$.

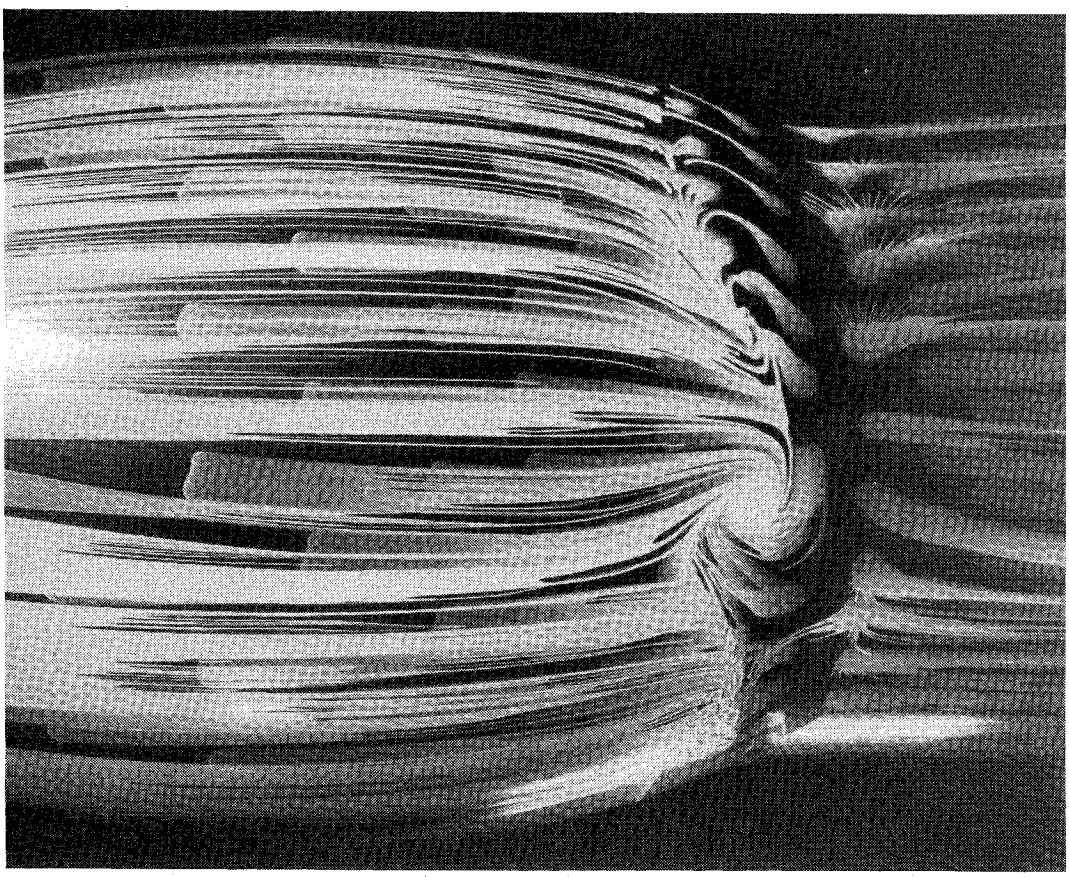

Fig. 2b Oil-flow visualization, $M = 0.8$.

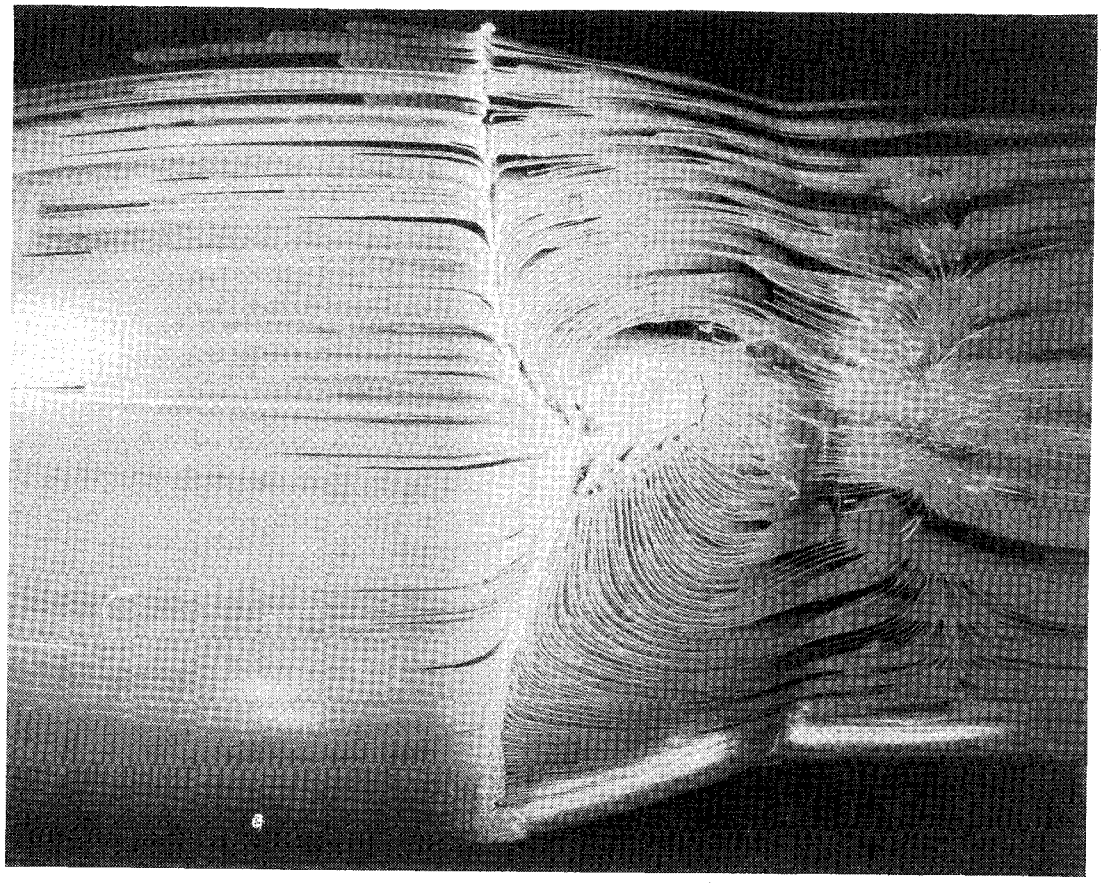

Fig. 2c Oil-flow visualization, $M = 0.862$.

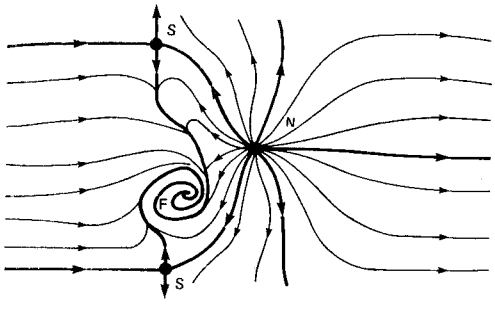

Fig. 2d Surface flow topography, $M = 0.7$.

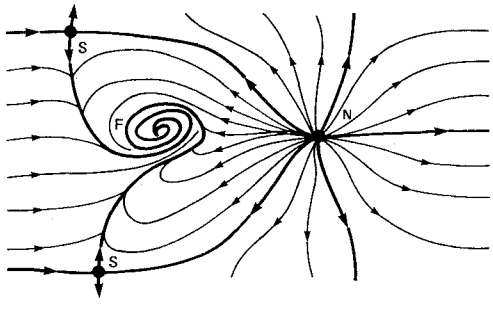

Fig. 2f Surface flow topography, $M = 0.862$.

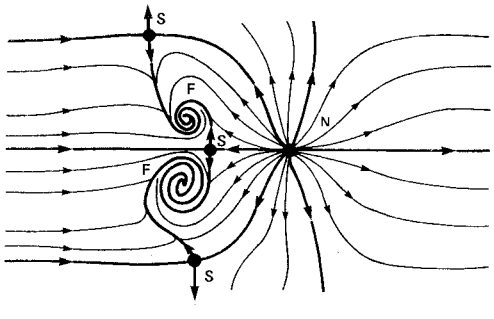

Fig. 2e Surface flow topography, $M = 0.8$.

The typical operating tunnel conditions for the data presented in this paper are summarized in Table 1. In the absence of the effects of the vortex, the adverse pressure gradient near the back end of the bump produced a small, nominally two-dimensional separation at the precritical Mach number. At the postcritical Mach number, the shock wave, together with the downstream pressure gradient, caused the boundary layer to separate two-dimensionally just downstream of the bump apex. At these Reynolds numbers, the straight section of the cylinder permitted natural transition in the boundary layer although in the present case, the vortex generator band probably also helped in triggering transition.

Results and Discussion

Surface Oil-Flow Visualization

The qualitative effect of the vortex on the separated boundary layer at three Mach numbers is illustrated in the surface oil-flow visualization photographs (Figs. 2a–2c). The

flow is from left to right, and the vortex is rotating in a clockwise direction when viewed from downstream. At a precritical Mach number of 0.7, the effect of the vortex was to delay the boundary-layer separation on the downwash side (vortex flow towards the surface) and move it somewhat forward on the upwash side (Fig. 2a). The resulting distorted separation line then formed a clockwise-rotating focus on the surface. When the Mach number was increased to that just below the critical 0.8, another focus appeared on the surface with a counter-clockwise rotation (Fig. 2b). With a further increase in Mach number, the separation moved upstream to the shock location, and at $M=0.862$, the counter-clockwise focus was found to dominate the surface flow pattern (Fig. 2c). At the postcritical Mach number, the separation is clearly delayed in the whole region of interaction, but asymmetrically, with maximum delay on the downwash side of the vortex. The reattachment was also found to be affected; it moved upstream in the region of the vortex at all three Mach numbers. In the absence of the vortex, the separation and reattachment lines in each case were found to be straight and symmetric all the way around the model.

At all the Mach numbers investigated, the main effect of the vortex was to transform a nominally two-dimensional separation into a three-dimensional one. A useful way to identify and characterize three-dimensional separated flows is by studying their topological features.[14] The surface flow topography for each of the present three-dimensional separations was derived from careful examination of the oil-flow pattern and by applying the topological rule[14] that the number of nodes (nodes points and foci) exceeds the number of saddle points by two. The topography for each of the three Mach numbers, 0.7, 0.8, and 0.862, is presented in Figs. 2d–2f, respectively. Each topography consists of at least one inward-spiraling separation focus (the surface flow feeds into the center) and a reattachment node, defined by the migration of surface flow away from it. The additional focus in Fig. 2e is complemented by the appearance of another saddle connecting the two foci. Note that the nodal points at the front and back ends of the model, corresponding to the flow attachment and detachment points, are not shown in these sketches. Although the three-dimensional separations appear to be well defined, the role of the vortex in producing them, and the drastic effect of the Mach number, are not easily understood. Some results from

Table 1 Summary of typical operating conditions

Case	Mach number	U, m/s	Reynolds number per meter
Precritical	0.7	230	12.5 million
Critical	0.8	260	13.5 million
Postcritical	0.862	280	13.75 million

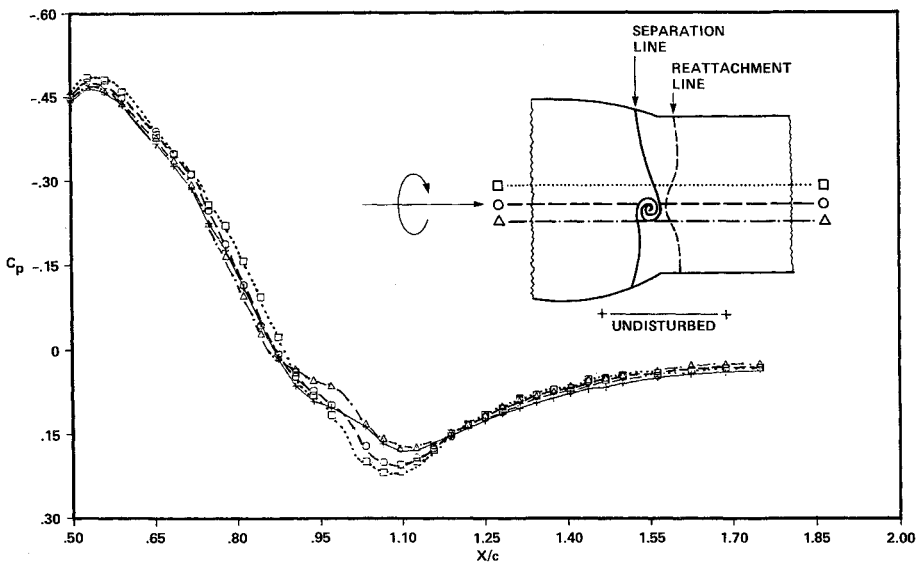

Fig. 3a Streamwise surface pressure distributions, $M=0.7$.

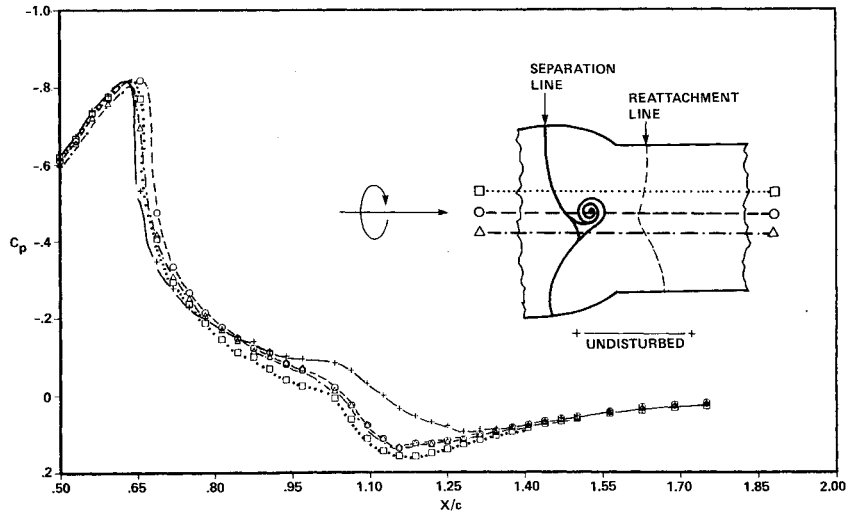

Fig. 3b Streamwise surface pressure distributions, $M=0.862$.

previous experiments on related topics may, however, help in explaining the observed effects.

The boundary layer approaching the separation consists of an imbedded longitudinal vortex. Previous studies[2,4] have shown that the local effect of the vortex is to thin the boundary layer (and hence increase the surface shear stress) on the downwash side and to thicken it somewhat on the upwash side. A small secondary streamwise vortex of opposite sign to the main vortex is also generated on the upwash side.[8] At the precritical Mach number, this boundary layer, with a spanwise-varying ability to negotiate a given adverse pressure gradient, separates asymmetrically, thus generating a focus on the surface, of the same sign as the main vortex (as viewed from downstream). At the postcritical Mach number, it seems that the effect of the vortex is to perturb the inherently unstable and unsteady shock wave/boundary-layer interaction such that the shock wave and the ensuing separation are moved downstream. Once again, the locally asymmetric separation forms a focus, but this time apparently adopting the sign of the secondary streamwise vortex, opposite to that of the main vortex. The "node/saddle" behavior in the shock/boundary-layer separation in a compression corner reported by Settles et al.[15] was probably due to a similar effect, the longitudinal vortices being generated by the Taylor-Goertler instability in the concave turn. The present flow visualization results are also qualitatively similar to those obtained in a vortex/wing study,[16] where the observed and conjectured surface flow patterns went through a similar change in the number and sign of surface foci as the angle of attack of the main wing was increased from zero to the stall angle.

Surface Pressure Measurements

Streamwise surface pressures at three spanwise or circumferential positions and at two Mach numbers are presented in Figs. 3a and 3b. Note that in these and subsequent figures, the curves are drawn for visual aid only. A schematic of the oil-flow photo is also included to illustrate the approximate profile locations. The undisturbed values shown on these and subsequent figures are those obtained with the vortex positioned at an orientation (90 deg to the measurement plane) where it was not expected to affect the flow in the measurement plane. This assumption was confirmed by comparing measurements made at the postcritical Mach number with those obtained by Bachalo and Johnson.[9]

For the precritical case, it is apparent from Fig. 3a that the maximum effect on the streamwise and spanwise pressures occurs in the region of the separation ($X/c \sim 1.0$). The pressures over the back of the bump ($0.5 \leq X/c \leq 1.0$) are also affected somewhat whereas those downstream of the reattachment ($X/c \geq 1.25$) seem to collapse reasonably well on the undisturbed curve. The pressure distributions confirm the implications of the oil-flow results, namely that the reversed-flow region is reduced substantially on the downwash side of the vortex while it is enhanced somewhat and moved upstream on the upwash side. Another interesting feature is that the spanwise pressure gradient changes sign, from negative at the upstream end of the separation ($X/c = 0.844$) to positive at the downstream end ($X/c = 1.031$).

For the postcritical case (Fig. 3b), the pressure results also confirm the implications of the oilflow visualization, namely that the shock position and the ensuing separation have been moved further downstream in the whole region of interaction with the vortex, although the shock strength does not seem to be affected significantly in this region. Following two-dimensional arguments and associating the maximum adverse pressure gradient downstream of the separation with the reattachment zone, it can be seen that the reattachment has also moved upstream, especially on the downwash side of the vortex. Note that this has resulted in a higher adverse pressure gradient in the reattachment region. This is consistent with the observations of Westphal and Johnston,[17] who found that for two-dimensional backward-facing step flows, the pressure coefficient scaled with the reattachment length such that the adverse pressure gradient was higher when the reattachment length was shortened. They also found that the reattachment length could be significantly shortened by installing vortex generators on the surface upstream of the separation point. So the overall effect of the vortex in the present case is to reduce the extent of the reversed-flow region by converting a two-dimensional separation into a three-dimensional one, although the surface pressure be-

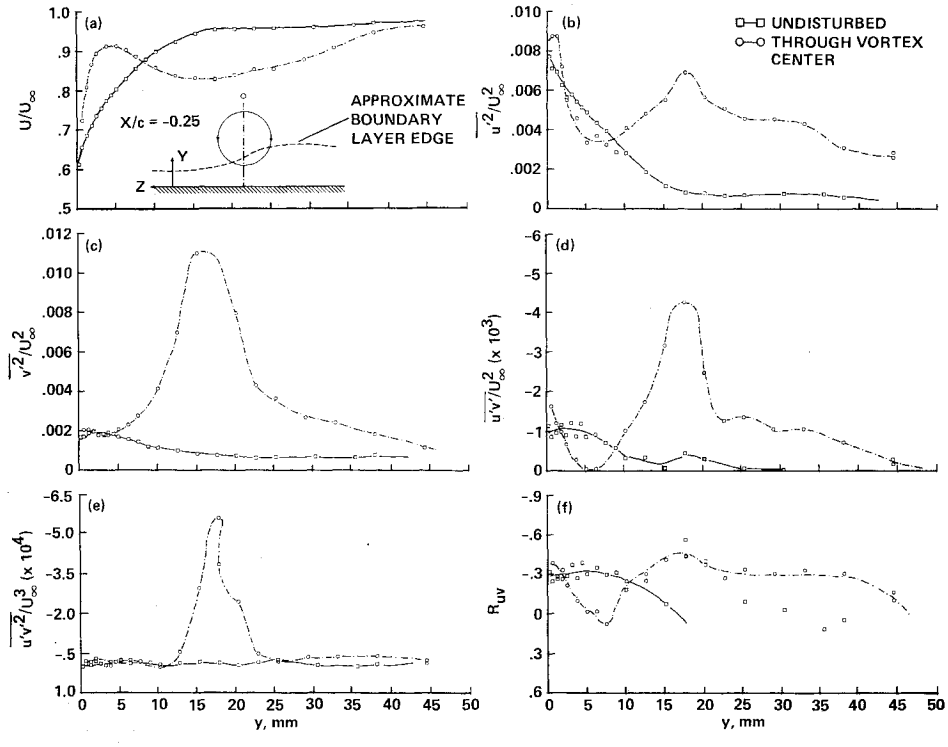

Fig. 4 Mean flow and turbulence profiles at $X/c = -0.25$, upstream of the bump, $M = 0.7$.

havior may still be explained using two-dimensional observations and arguments.

Mean Flow and Turbulence Measurements Upstream of the Bump

Some details of the undisturbed boundary layer and the generated vortex were characterized by measuring two profiles upstream of the bump at $X/c = -0.25$. Since the results at this location for both Mach numbers were qualitatively similar, only one set ($M = 0.7$) is presented here (Figs. 4a–4f). A turbulent boundary layer ($\delta_{995} \sim 1.7$ cm) was obtained at the bump leading edge. Associating the dip in the mean velocity profile and the peak in the turbulence profiles with the core position, the vortex is centered approximately at the edge of the undistributed boundary layer, as was intended by design.

The core region of the vortex is obviously turbulent, with higher levels of Reynolds normal and shear stress than in the boundary layer. The maximum stress levels in the core region for the postcritical case were somewhat lower, comparable to the maximum levels in the boundary layer. Two-dimensional criteria suggest that the core flow in a vortex is highly stable and so any turbulence present there should decay rapidly. However, this is not found to be the case in practical three-dimensional flows with axial velocity such as the present one.[18] In fact, previous studies[19] have suggested that, under certain circumstances, the vortex may even produce turbulence. The mechanism by which a vortex of this type generates turbulence within the core region is by first acquiring normal stresses ($\overline{u'^2}$, $\overline{v'^2}$, $\overline{w'^2}$), through, for example, remnants of the generator wake or entrainment of boundary-layer fluid. The generation of shear stresses would then result from the interaction of the normal stresses with the appropriate mean rate-of-strain; the dominant production term for $\overline{u'v'}$ is $\overline{v'^2}(\partial U/\partial Y)$. The triple product ($\overline{u'v'^2}$), which represents turbulent diffusion of Reynolds stress, also shows a high peak in the vortex. The shear correlation coefficient R_{uv}, which is useful in identifying structural changes, shows values in the vortex of the same order as those found in the boundary layer. Note that normally the actual values of R_{uv} in the region beyond the boundary layer are ratios of small measured quantities and hence not very accurate. However, in the present case, the vortex has significant stresses in the core region which seem to be well correlated. So the flow upstream of the bump consists of a turbulent boundary layer in equilibrium with a turbulent vortex located near its outer edge.

Mean Flow and Turbulence Measurements in the Separated Region

Data for the pre- and postcritical Mach numbers are presented in Figs. 5 and 6 for the station located at the back end of the bump, where the reversed-flow region was the largest ($X/c = 1.0$). Measurements at other stations in the separated region showed similar trends for both Mach numbers; these measurements, together with some results obtained in the reattachment region, are given in Refs. 10 and 11.

Figures 5a–5f show the profiles measured at $X/c = 1.0$ for $M = 0.7$. The mean profiles show that the streamwise velocity near the surface is increased in the whole region of interaction and imply that the boundary layer is thinned on the downwash side of the vortex and thickened on the upwash side. In agreement with previous subsonic data,[20] the undisturbed separated boundary-layer profiles exhibit high levels of Reynolds stress with maxima near the middle of the layer. The qualitative effect of the vortex on all of the turbulence quantities is consistent with the observations made earlier. In particular, the Reynolds-stress maxima are increased significantly on the upwash side of the vortex, where the separation effects (reversed-flow region) are enhanced, and are reduced somewhat on the downwash side, where the effects are suppressed. The turbulence transport and structural terms are affected in a similar manner. Although the shear stress peak is somewhat lower in the vortex core region compared to the profile at $X/c = -0.25$, the two normal stresses have retained their relatively high magnitudes. Transport of the shear stress in the core region is minimal, but relatively high values of the shear correlation coefficient are again indicated in this region.

The data for the postcritical case are plotted as contour plots with the circular cross section unfolded and the individual profiles straightened (Figs. 6a–6f). Although the in-

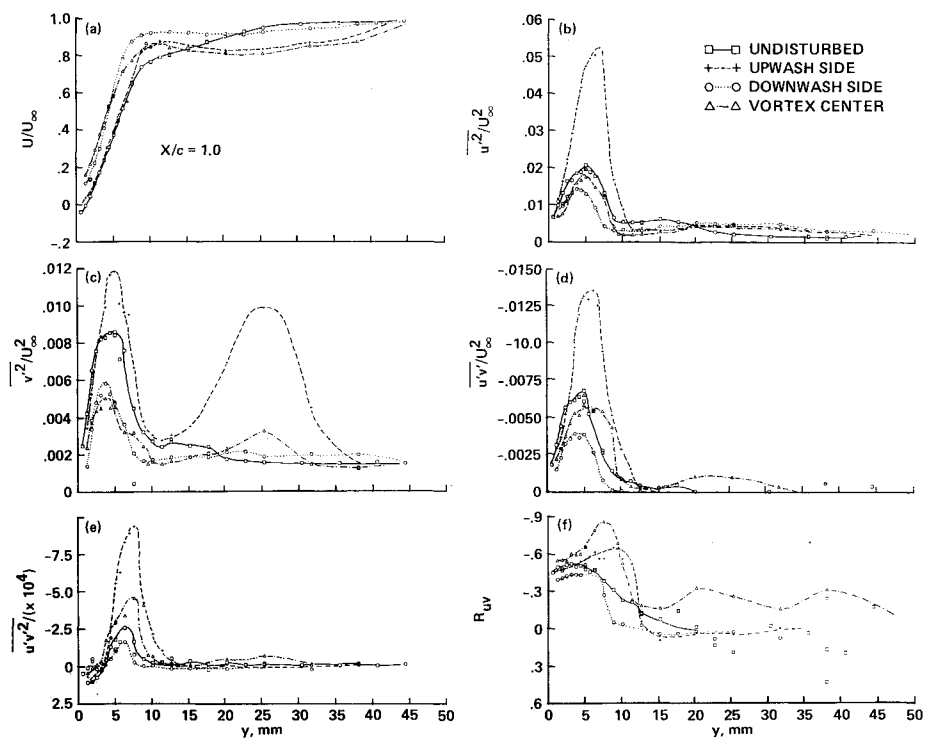

Fig. 5 Mean flow and turbulence profiles at $X/c = 1.0$, in the separated region at the downstream end of the bump, $M = 0.7$.

dividual profiles were measured perpendicular to the surface, unfolding in this manner does not produce a significant distortion of the contours since the total included angle of the spanwise profiles plotted is only about 35 deg. The approximate position of the vortex center, as determined from the mean velocity data, is sketched on these plots for reference, and the flow is going into the plane of the paper.

The mean streamwise velocity contours in the separated region at $X/c=1.0$ are presented in Fig. 6a. The outermost contours indicate that the vortex may have entrained some boundary-layer material, although contour levels below 0.8 only seem to indicate an overall reduction in boundary-layer thickness. The other main features evident in this plot are the reduction in the size of the reversed-flow region near the wall, compared to the undistributed case, and higher reductions in the negative velocity directly underneath the vortex.

The results for the Reynolds-stress components, $\overline{u'^2}$, $\overline{v'^2}$, and $\overline{u'v'}$ in the separated region are presented in Figs. 6b–6d. Since the retained-stress levels in the core region are now very small compared to those in the separated layer, the vertical axes on the turbulence quantity plots have been expanded. Once again, the undisturbed separated boundary-layer profiles exhibit high levels of Reynolds stress, with maxima near the middle of the layer. Note that a shock-induced separation produces a turbulence flow structure similar to that for an incompressible separated flow,[20] so direct comparison is justified. The vortex causes severe distortion of the contours, especially on the downwash side. The effect of the vortex is apparent for relatively large spanwise distances—total recovery to the undisturbed levels is not observed within the measurement plane (~4–5 shear-layer thicknesses). The separated boundary-layer thickness, assessed from turbulence stress levels, is also reduced throughout the measurement plane. The peak levels of Reynolds stress have been reduced, particularly on the downwash side of the vortex, where the reduction is by almost a factor of two. The peaks are also moved closer to the wall, as would be expected, since the shear-layer thickness is now reduced. In addition, the stress levels near the wall have been increased. The turbulence transport (Fig. 6e) and structural terms (Fig. 6f) have also been grossly affected by the vortex, with significant reductions on the downwash side.

The mean and turbulent properties of the boundary layer in the separated region have been reorganized significantly by the vortex at both Mach numbers. The overall effect of the vortex is to increase the distribution of mean streamwise

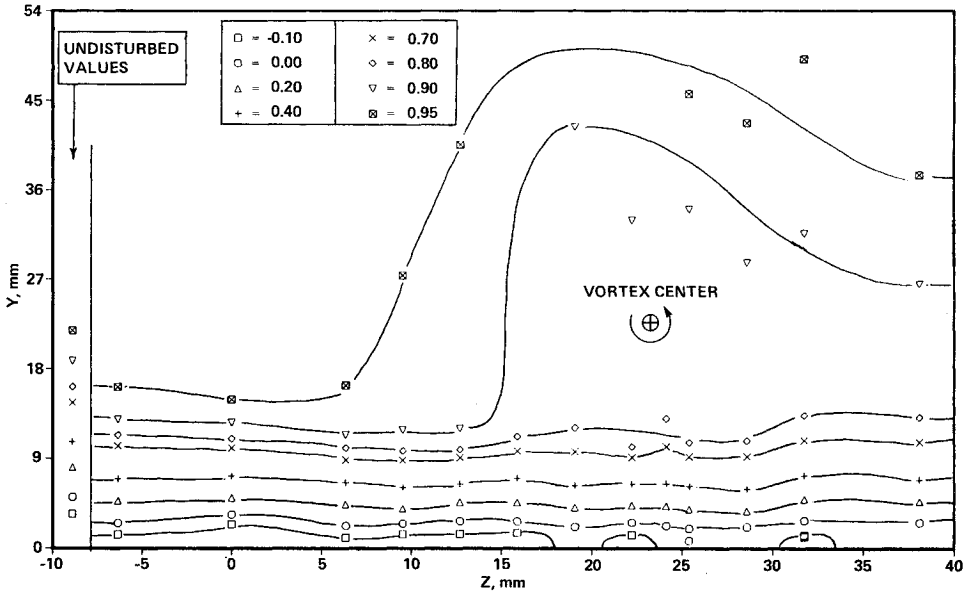

Fig. 6a Mean velocity (U/U_∞) contours at $X/c=1.0$, in the separated region at the downstream end of the bump, $M=0.862$.

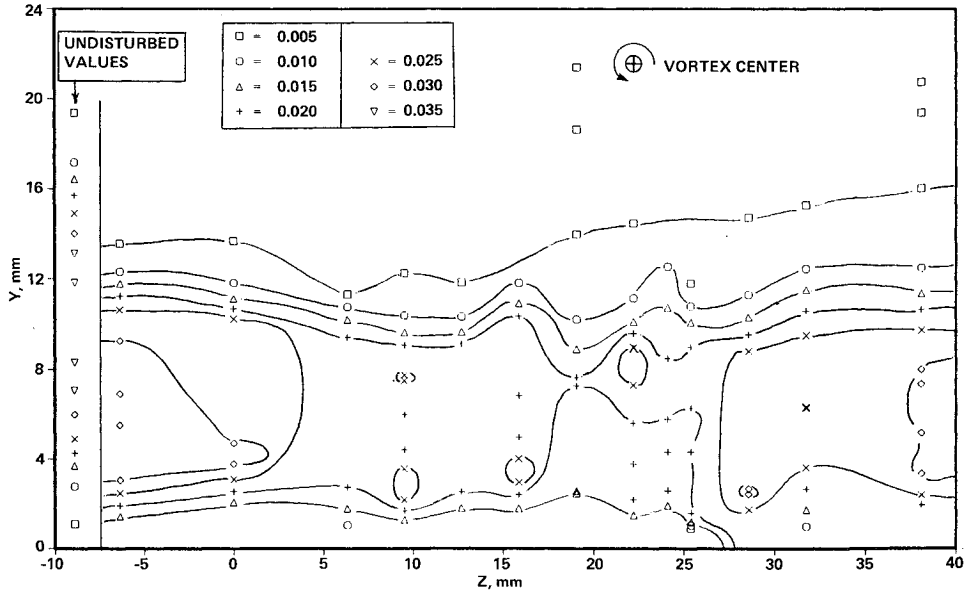

Fig. 6b Streamwise fluctuation ($\overline{u'^2}/U_\infty^2$) contours at $X/c=1.0$, in the separated region at the downstream end of the bump, $M=0.862$.

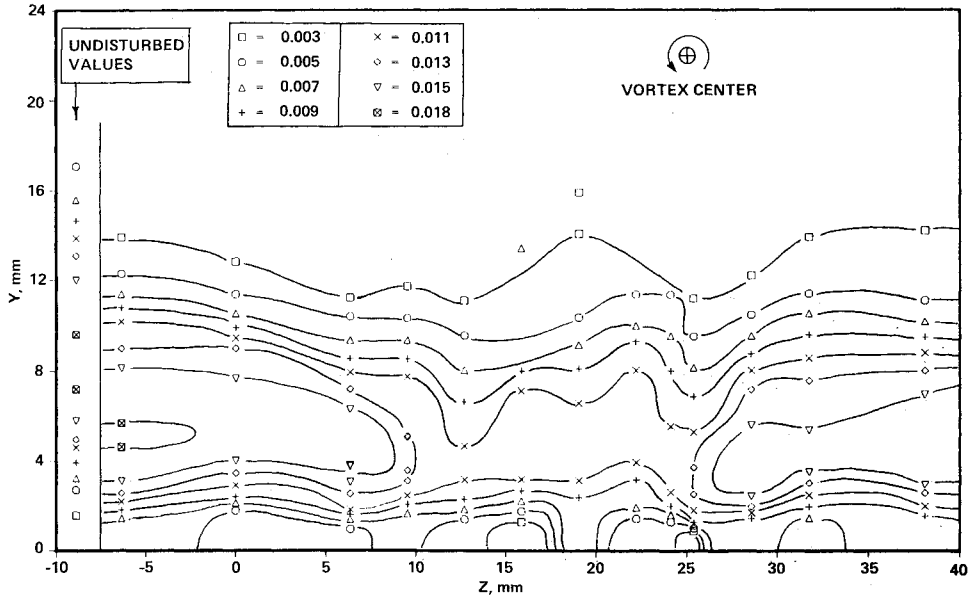

Fig. 6c Normal fluctuation ($\overline{v'^2}/U_\infty^2$) contours at $X/c = 1.0$, in the separated region at the downstream end of the bump, $M = 0.862$.

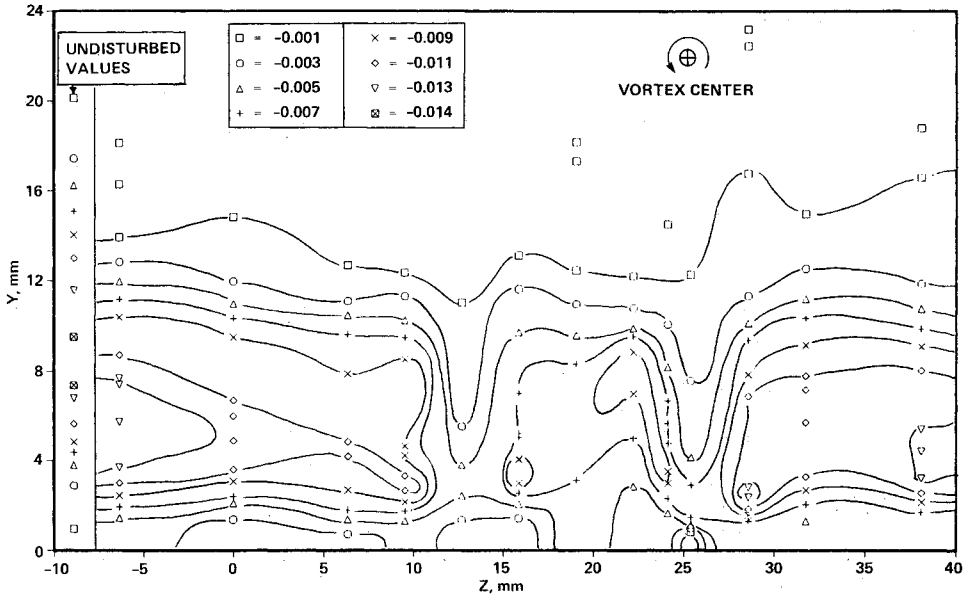

Fig. 6d Primary shear stress ($\overline{u'v'}/U_\infty^2$) contours at $X/c = 1.0$, in the separated region at the downstream end of the bump, $M = 0.862$.

velocity near the surface, thus reducing the reversed-flow region and hence, the separation effects. At the precritical Mach number, the asymmetric (three-dimensional) separation leads to asymmetric distributions of the Reynolds stresses. The effect of the vortex at postcritical Mach number is to reduce the region of reversed flow by delaying separation in the whole region of interaction and moving the reattachment upstream. The growth of the separated shear layer is also inhibited since the main action of an embedded vortex is to transport relatively high-momentum fluid toward the surface, thus increasing the overall surface shear stress.[2,4] This means that the extent of separation has been reduced and this is reflected in the increase in mean streamwise velocity near the surface and underneath the vortex. A smaller separation would also imply lower Reynolds stress peaks since the separated shear layer has not grown as much, and this is indeed the case, as seen in Figs. 6b–6d.The higher levels of Reynolds stress near the wall also indicate that the boundary layer is now closer to recovery. The qualitative behavior of the separated boundary layer is perhaps not too difficult to follow, assuming quasi-two-dimensional behavior, but the quantitative redistribution of the stresses is rather complex, with large spanwise variations. The maximum reductions in stresses occur on the downwash side of the vortex, at least partly due to the transfer of high-momentum fluid toward the wall.

While the detailed behavior of the turbulence in this three-dimensional flow cannot be assessed without the cross-plane measurements, application of simple similarity laws (established for two-dimensional separated boundary layers) helps in determining departure from "equilibrium." For example, Simpson et al.[21] showed that a two-dimensional separated boundary layer soon reaches a form of self-similarity where the maximum streamwise normal stress scales on the distance of the peak from the wall. In the present results, while the peak stress levels in the spanwise direction for both Mach numbers are altered by up to 30%, the distance of the peak from the wall is not affected as much, and so the proposed self-similarity would not be satisfied. Another indication of the level of perturbation can be obtained by examining the validity of some turbulence models. The simpler turbulence models are all based on eddy viscosity, defined as the ratio of shear stress to the corresponding mean rate of strain $[= \overline{u'v'}/(\partial U/\partial Y)]$ for a two-dimensional shear flow. In a separated boundary layer, however, the shear stress should ideally be modeled by relating it to turbulence structure rather than to the local mean velocity gradient.[20] On investigating the behavior of the eddy viscosity, Simpson et al.[22] found that while its actual levels were lower in the separated region, the profiles exhibited similarity for the various streamwise locations (when δ_{995} was used to scale Y) in the outer layer as well near the wall. Although the eddy viscosity was not evaluated specifically in

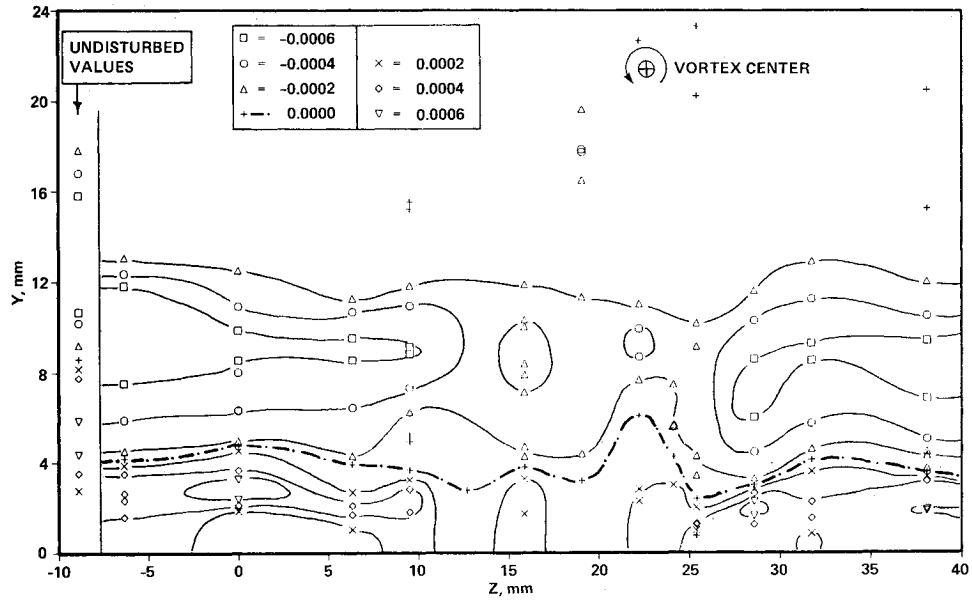

Fig. 6e Turbulence transport ($\overline{u'v'^2}/U_\infty^3$) contours at $X/c=1.0$, in the separated region at the downstream end of the bump, $M=0.862$.

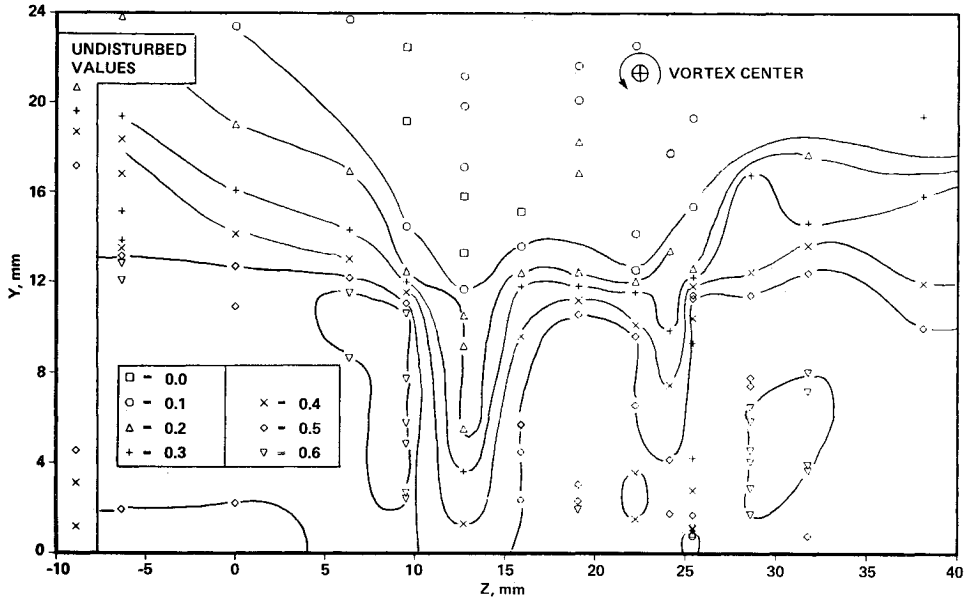

Fig. 6f Turbulence structure (R_{uv}) contours at $X/c=1.0$, in the separated region at the downstream end of the bump, $M=0.862$.

the present investigation, it is clear that this quantity will not be well-behaved at either Mach number. For instance, in the postcritical case, while the mean streamwise velocity (and hence its derivative) in the main part of the boundary layer is well-behaved in the spanwise direction, $\overline{u'v'}$ varies considerably. The distribution of this component of the eddy viscosity at this station would therefore have a very complex behavior in the spanwise direction.

The fact that such similarity is not satisfied in the spanwise direction indicates that the present interaction is not just a two-dimensional flow which has been simply distorted by the vortex such that all the turbulence parameters scale on the local boundary-layer thickness, thus retaining certain equilibrium properties. Obviously, three-dimensional effects are now also playing an important role in the behavior of this turbulent flow. For example, the secondary flow due to the vortex is bound to affect the orientation of the turbulent eddies and hence contributions to the shear stresses, besides also affecting the turbulence transport directly. Hence, higher-order turbulence models would probably be required if this flow were to be computed accurately. This obviously means the higher-order turbulence quantities would have to be modeled accurately, in addition to the shear stress.

Triple products of velocity fluctuations appear in the turbulent-transport terms of the transport equations for turbulent energy and shear stress and are determined mainly by the large eddies. In the separated region, the undisturbed profiles for $\overline{u'v'^2}$ indicate a transport of $-\overline{u'v'}$ away from the wall in the outer layer. This is in agreement with Simpson et al.'s[23] measurements in a two-dimensional separating boundary layer, where they found an increasingly strong transport of turbulent kinetic energy away from the wall in the outer region. In fact, they proposed that this diffusion was responsible for the rapid growth of separated boundary layers. The undisturbed profiles in the present case also indicate a large positive region near the surface. Turbulence transport is known to be toward the wall in the inner layer of boundary layers which contain shear-stress peaks caused by adverse pressure gradients.[23,24] The effect of the vortex on turbulence transport in the outer region may be explained, at least qualitatively, by convection effects due to the secondary flow, so that transport of $-\overline{u'v'}$ away from the wall is decreased on the downwash side. For the postcritical case, the region of positive $\overline{u'v'^2}$ has been reduced throughout the cross-stream plane, with smaller values on the downwash side of the vortex. The reduction in positive $\overline{u'v'^2}$ is consis-

tent with the reduction in shear stress peaks and separation effects. In the precritical case, there is an *increase* in *positive* $\overline{u'v'^2}$ near the wall on the upwash side of the vortex. This does not correspond to a negative gradient or any noticeable feature of $\overline{u'v'}$ and could be a natural response of the inner-layer turbulence when convected away from the surface by the vortex. A similar behavior of this triple product was also observed in the vortex/boundary-layer study.[2] Hence, the overall behavior of this quantity is far from simple, and the task of developing empirical models for it appears rather daunting.

The shear correlation coefficient in the current undisturbed boundary layer in the separated region is well-behaved, with a constant value over a significant part of the boundary layer, as was also observed by Simpson et al.[21] However, the vortex affects the R_{uv} distribution significantly, with some regions of "overshoot" where R_{uv} is increased over the maximum undisturbed value. The overshoot in R_{uv} is often encountered in perturbed boundary layers and normally suggests an increased activity leading to reorganization of the large, shear-stress-producing eddies and hence enforcing rapid recovery.[24,25] So the action of the vortex is to modify and reorganize, but not destroy, the structure of the boundary-layer turbulence.

Conclusions

The interaction between a longitudinal vortex and a separated boundary layer has been studied experimentally at three transonic Mach numbers. As expected, the overall effect of the vortex is to reduce the region of reversed flow by transfering higher-momentum fluid toward the wall. However, the redistribution of the mean flow and turbulence quantities is rather complicated, with large spanwise changes which cannot all be explained in terms of a simple distortion of the initially two-dimensional flow.

At precritical speeds, the vortex delays or eliminates boundary-layer separation on the downwash side and enhances it on the upwash side, thus producing an asymmetric, three-dimensional separation. At postcritical speeds, the overall effect of the vortex is to reduce the level and region of boundary-layer separation throughout the region of interaction. The vortex delays separation by perturbing the already unstable shock wave/boundary-layer interaction such that it moves downstream. The growth of the separated shear layer is then inhibited by the vortex, and reattachment occurs sooner. The boundary-layer turbulence at both speeds is found to reorganize accordingly, although the detailed distribution is not easy to follow. The simpler turbulence models are therefore not expected to work very well for these types of interactions. Furthermore, the behavior of the higher-order terms indicates that the implementation of more sophisticated models may not be straightforward either.

The generated vortex perturbs the separation line and introduces three-dimensionality which generates secondary vortices or foci on the surface, the sign and number being dependent on the Mach number. So, both qualitatively and quantitatively, there are substantial Mach number effects, especially when the crtical Mach number is crossed. It should be noted that the longitudinal vortices used to control boundary-layer separation in practice may be much stronger than the one used in the present study, and hence the actual interaction should be expected to be even more complex and more three-dimensional.

Acknowledgments

This research project was conducted in the Fluid Dynamics Research Branch at NASA Ames Research Center while the author was on a National Research Council Associateship. Helpful comments by Dennis A. Johnson during the course of this study are gratefully acknowledged. I am grateful to Alexander J. Smits for pointing out the relevance of Ref. 15 to this work and to Russell V. Westphal, Stephen K. Robinson, and Murray Tobak for many helpful suggestions on an earlier draft of this article. The LDV data were taken with the help of personnel from Complere Incorporated.

References

[1]"Proceedings, 1980-81, AFOSRHTTM-Stanford Conference on Complex Turbulent Flows, Vol. 2, edited by S. J. Kline, B. J. Cantwell, and G. M. Lilley, 1982.

[2]Shabaka, I. M. M. A., Mehta, R. D., and Bradshaw, P., "Longitudinal Vortices Imbedded in Turbulent Boundary Layers, Part I—Single Vortex," *Journal of Fluid Mechanics*, Vol. 155, June 1985, pp. 37-57.

[3]Liandrat, J., Aupoix, B., and Cousteix, J., "Calculation of Longitudinal Vortices Imbedded in a Turbulent Boundary Layer," *Proceedings of the Fifth Symposium on Turbulent Shear Flows*, Cornell Univ., Ithaca, NY, 1985; Springer-Verlag, NY, 1986.

[4]Westphal, R. V., Eaton, J. K., and Pauley, W. R., "Interaction Between a Vortex and a Turbulent Boundary Layer in a Streamwise Pressure Gradient," *Proceedings of the Fifth Symposium on Turbulent Shear Flow*, Cornell Univ., Ithaca, NY, Aug. 1985; Springer-Verlag, NY, 1986.

[5]Westphal, R. V. and Mehta, R. D., "Interaction of an Oscillating Vortex with a Turbulent Boundary Layer," AIAA Paper 87-1246, June 1987.

[6]Leibovich, S., "Vortex Breakdown and Stability: Survey and Extension," *AIAA Journal*, Vol. 22, Sept. 1984, pp. 1192-1206.

[7]Delery, J., Horowitz, E., Leuchter, O., and Solignac, J. L., "Fundamental Studies on Vortex Flows," *La Recherche Aerospatiale*, Vol. 2, 1984, pp. 1-24.

[8]Staff, Fluid Dynamics Research Branch, "Vortical Flows Research Program of the Fluid Dynamics Research Branch," NASA-TM 88332, Aug. 1986.

[9]Bachalo, W. D. and Johnson, D. A., "An Investigation of Transonic Turbulent Boundary Layer Separation Generated on an Axisymmetric Flow Model," *AIAA Journal*, Vol. 24, March 1986, pp. 437-443.

[10]Mehta, R. D., "Effect of a Longitudinal Vortex on a Separated Turbulent Boundary Layer," AIAA Paper 85-0530, March 1985.

[11]Mehta, R. D., "Interaction Between a Longitudinal Vortex and a Shock-Induced Turbulent Boundary Layer Separation," AIAA Paper 86-0346, Jan. 1986.

[12]Horstman, C. C. and Johnson, D. A., "Prediction of Transonic Separated Flows," *AIAA Journal*, Vol. 22, July 1984, pp. 1001-1003.

[13]Johnson, D. A., Modarress, D., and Owen, F. K., "An Experimental Verification of Laser-Velocimeter Sampling Bias and its Correction," *ASME Journal of Fluids Engineering*, Vol. 106, 1984, pp. 5-12.

[14]Tobak, M. and Peake, D. J., "Topology of Three-Dimensional Separated Flows," *Annual Review of Fluid Mechanics*, Vol. 14, 1982, pp. 61-85.

[15]Settles, G. S., Fitzpatrick, T. J., and Bogdonnoff, S. M., "Detailed Study of Attached and Separated Compression Corner Flowfields in High Reynolds Number Supersonic Flow," *AIAA Journal*, Vol. 17, June 1979, pp. 579-585.

[16]Mehta, R. D. and Lim, T. T., "Flow Visualization Study of a Vortex/Wing Interaction," NASA-TM 86656, 1984.

[17]Westphal, R. V. and Johnston, J. P., "Reattaching Turbulent Shear Layers with Perturbed Structure," *AIAA Journal*, Vol. 22, Dec. 1984, pp. 1727-1731.

[18]Phillips, W. R. C. and Graham, J. A. H., "Reynolds-Stress Measurements in a Turbulent Trailing Vortex," *Journal of Fluid Mechanics*, Vol. 147, 1984, pp. 353-371.

[19]Mehta, R. D., "An Experimental Study of a Vortex/Mixing Layer Interaction," AIAA Paper 84-1543, June 1984.

[20]Simpson, R. L., "Some Features of 2-D Turbulent Separated Flows," AIAA Paper 85-0178, Jan. 1985; see also "2-D Turbulent Separated Flows," AGARDograph 287, Vol. 1, 1985.

[21]Simpson, R. L., Strickland, J. H., and Barr, P. W., "Features of a Separating Turbulent Boundary Layer in the Vicinity of Separation," *Journal of Fluid Mechanics*, Vol. 79, 1977, pp. 553-594.

[22]Simpson, R. L., Chew, Y. T., and Shivaprasad, B. G., "The Structure of a Separating Turbulent Boundary Layer. Part 1. Mean Flow and Reynolds Stresses," *Journal of Fluid Mechanics*, Vol. 113, 1981, pp. 23–51.

[23]Simpson, R. L., Chew, Y. T., and Shivaprasad, B. G., "The Structure of a Separating Turbulent Boundary Layer. Part 2. Higher-Order Turbulence Results," *Journal of Fluid Mechanics*, Vol. 113, 1981, pp. 53–73.

[24]Smits, A. J., Young, S. T. B., and Bradshaw, P., "The Effect of Short Regions on High Surface Curvature on Turbulent Boundary Layers," *Journal of Fluid Mechanics*, Vol. 94, 1979, p. 209.

[25]Mehta, R. D., "Aspects of the Design and Performance of Blower Tunnel Components," Ph.D. Thesis, Aeronautics Dept., Imperial College, London Univ., UK, 1978.